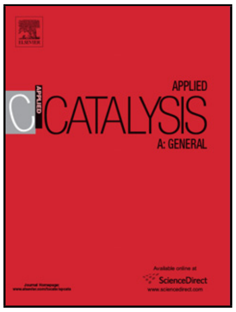

Title: Palladium-DABCO complex supported on γ-Fe_2O_3 magnetic nanoparticles: A new catalyst for C–C bond formation *via* Mizoroki-Heck cross-coupling reaction

Author: Sara Sobhani Zahra Pakdin-Parizi

PII: S0926-860X(14)00269-5
DOI: http://dx.doi.org/doi:10.1016/j.apcata.2014.04.028
Reference: APCATA 14801

To appear in: *Applied Catalysis A: General*

Received date: 14-12-2013
Revised date: 14-4-2014
Accepted date: 15-4-2014

Please cite this article as: S. Sobhani, Palladium-DABCO complex supported on *rmgamma*-Fe_2O_3 magnetic nanoparticles: A new catalyst for C-C bond formation *via* Mizoroki-Heck cross-coupling reaction, *Applied Catalysis A, General* (2014), http://dx.doi.org/10.1016/j.apcata.2014.04.028

*Graphical Abstract (for review)

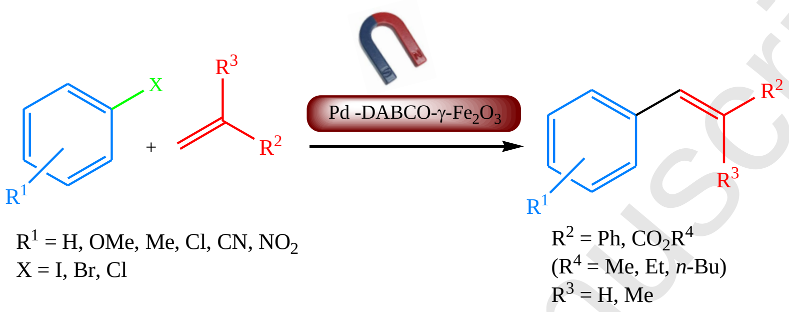

Research Highlights:

- Palladium-DABCO complex supported on γ-Fe_2O_3 (Pd-DABCO-γ-Fe_2O_3) was synthesized.
- Pd-DABCO-γ-Fe_2O_3 is a new phosphine-free palladium catalyst.
- Pd-DABCO-γ-Fe_2O_3 was successfully applied in Mizoroki-Heck cross-coupling reaction.
- Pd-DABCO-γ-Fe_2O_3 was isolated from the reaction mixture by magnetic decantation.

Palladium-DABCO complex supported on γ-Fe_2O_3 magnetic nanoparticles: A new catalyst for C-C bond formation *via* Mizoroki-Heck cross-coupling reaction

Sara Sobhani,* Zahra Pakdin-Parizi

Department of Chemistry, College of Sciences, University of Birjand, Birjand, Iran

*Corresponding author. Tel. +98 (561) 2502065; Fax: +98 (561) 2502065

E-mail address: ssobhani@birjand.ac.ir, sobhanisara@yahoo.com

Abstract

In this paper, palladium-DABCO complex supported on γ-Fe_2O_3 magnetic nanoparticles (Pd-DABCO-γ-Fe_2O_3) was synthesized and characterized by HRTEM, SEM, XRD, XPS, ICP, FT-IR, TGA, VSM and elemental analysis. The synthesized catalyst was successfully applied as a new magnetically recyclable heterogeneous catalyst in Mizoroki-Heck cross-coupling reaction of aryl halides with alkyl acrylates and styrene under solvent-free conditions.

Keywords: Palladium, Magnetic nanoparticle, Heterogeneous catalyst, Mizoroki-Heck, DABCO

1. Introduction

Palladium is one of the most crucial metals in catalysis and it is commonly used to catalyze a large variety of carbon–carbon (Csp^2-Csp^2) bond forming reactions [1-4]. Among these reactions, palladium-catalyzed arylation of olefins, the Mizoroki-Heck cross-coupling reaction, is an extremely useful and general technique for the synthesis of biologically active functionalized olefins [5-8]. These cross-coupling reactions are commonly catalyzed by homogeneous palladium complexes containing phosphine ligands. However, the soluble palladium phosphine complexes suffer from problems associated with the separation, recovery, and instability at high temperatures. Moreover, most of phosphine ligands are expensive, toxic, not easily available, sensitive to air and moisture [9-11]. Consequently, the development of new heterogeneous phosphine-free palladium catalysts is an ongoing challenge in this field of study [12-16].

1,4-Diazabicyclo[2.2.2]octane (DABCO) is a medium-hindrance tertiary amine with cage-like structure, which used as an inexpensive, eco-friendly, highly reactive and non-toxic ligand or catalyst for various organic transformations [17-20]. DABCO was also appeared as a substitute to phosphine ligands for the palladium-catalyzed Suzuki-Miyaura and Mizoroki-Heck cross-coupling reactions. Due to the importance of using heterogeneous catalysts, recently, palladium-DABCO complex supported on polymer, silica or SBA-15 was synthesized and used as solid catalysts for cross-coupling reactions [21-24]. Despite the high catalytic activity of these heterogeneous palladium catalysts, their separation techniques were energy and time consuming and caused loss of the catalyst. Immobilization of palladium-DABCO complex on magnetic nanoparticles (MNPs) offers a solution to this problem due to the ease of catalyst separation by applying an appropriate magnetic field. Magnetic separation of MNPs, which is an alternative to filtration or centrifugation, prevents loss of the catalyst, facilitates its recycling and saves time and energy. To benefit the valuable applications of MNPs and unique properties of DABCO as a ligand, and in continues of our recent works on the development of new heterogeneous catalysts [25-32], herein, we report the synthesis of palladium-DABCO complex supported on γ-Fe_2O_3 magnetic nanoparticles (Pd-DABCO-γ-Fe_2O_3). We have also used the synthesized Pd-DABCO-γ-Fe_2O_3 as a new magnetically recyclable heterogeneous catalyst for Mizoroki-Heck cross-coupling reactions under solvent-free conditions.

2. Experimental

Chemicals were purchased from Merck Chemical Company. NMR spectra were recorded in ppm in $CDCl_3$ on a Bruker Avance DPX-400 instrument using TMS as internal standard. The purity of the products and the progress of the reactions were accomplished by TLC on silica-gel polygram SILG/UV254 plates. HRTEM analysis were performed using HRTEM microscope (Philips CM30). The morphology of the products was determined by using Hitachi Japan, model s4160 Scanning Electron Microscopy (SEM) at accelerating voltage of 15 KV. FT-IR spectra were recorded on a JASCO FT-IR 460 plus spectrophotometer. Thermo gravimetric analysis (TGA) was performed using a Shimadzu thermo gravimetric analyzer (TG-50). Elemental analysis was carried out on a Costech 4010 CHNS elemental analyzer. Power X-ray diffraction (XRD) was performed on a Bruker D8-advance X-ray diffractometer or on a X'Pert Pro MPD diffractometer with Cu K_α (λ = 0.154 nm) radiation. Surface analysis spectroscopy of the catalyst were performed in an ESCA/AES system. This system was equipped with a concentric hemispherical (CHA) electron energy analyzer (Specs model EA10 plus) suitable for X-ray photoelectron spectroscopy (XPS). Room temperature magnetization isotherms were obtained using a vibrating sample magnetometer (VSM, LakeShore 7400). The content of Pd in the catalyst was detemined by OPTIMA 7300DV ICP analyzer.

2.1. Synthesis of γ-Fe_2O_3 MNPs

γ-Fe_2O_3 MNPs were synthesized by a reported chemical co-precipitation technique of ferric and ferrous ions in alkali solution with minor modifications [33,34]. $FeCl_2.4H_2O$ (1.99 g) and $FeCl_3.6H_2O$ (3.25 g) were dissolved in deionized water (30 mL) under Ar atmosphere at room temperature. A NH_4OH solution (0.6 M, 200 mL) was then added drop wise (drop rate = 1 $mL.min^{-1}$) to the stirring mixture at room temperature to reach the reaction pH to 11. The resulting black dispersion was continuously stirred for 1 h at room temperature, and heated to reflux for 1 h to yield a brown dispersion. The magnetic nanoparticles were subsequently separated by a magnetic bar and washed with deionized water until it was neutralized. The as-synthesized sample was heated at 2 $^{o}C.min^{-1}$ up to 250 ^{o}C and then kept in the furnace for 3 h to give a reddish-brown powder.

2.2. Synthesis of chloro-functionalized γ-Fe_2O_3

The prepared γ-Fe_2O_3 (3.6 g) was sonicated in dry toluene (50 mL) for 30 min. 3-chloropropyltrimethoxysilane (4 mL) and triethylamine (as a catalyst, 0.4 mL) was added to the dispersed γ-Fe_2O_3 in toluene, slowly heated to 105 °C and stirred at this temperature for 48 h. The resulting chloro-functionalized γ-Fe_2O_3 was separated by an external magnet and washed with toluene, ethanol-water mixture, deionized water and ethanol in turn, and dried under vaccum.

2.3. Synthesis of γ-Fe_2O_3 supported with DABCO (DABCO-γ-Fe_2O_3)

DABCO (2 g) was added to a magnetically stirred mixture of chloro-functionalized γ-Fe_2O_3 (3.6 g) in dry acetone (100 mL). After refluxing for 36 h, the mixture was cooled to room temprature. The resulting DABCO-γ-Fe_2O_3 was separated by an external magnet, washed with acetone and dried in oven under vaccum.

2.4. Synthesis of palladium-DABCO complex supported on γ-Fe_2O_3 (Pd-DABCO-γ-Fe_2O_3)

DABCO-γ-Fe_2O_3 (3.3 g) was added to a solution of palladium acetate (0.11 g) in dry acetone (30 mL). The reaction mixture was stirred at room temperature for 24 h. After stirring, the solid was separated by an external magnet, and washed with acetone, ethanol and ether. It was then dried in an oven at 90 °C overnight to furnish Pd-DABCO-γ-Fe_2O_3.

2.5. General procedure for heterogeneous Mizoroki-Heck cross-coupling reaction

A mixture of aryl halid (1 mmol), olefin (1.1 mmol), Et_3N (2 mmol) and catalyst (0.06 g, 1 mol%) was stirred at 100 °C for an appropriate time (Table 2). The reaction mixture was diluted with EtOAc. The catalyst was separated by an external magnet, washed with EtOAc, dried and re-used for a consecutive run under the same reaction conditions. Evaporation of the solvent of the filtrate under reduced pressure gave the crude products. The pure products were isolated by chromatography on silica gel eluted with *n*-hexane:EtOAc (50:1).

(E)-Methyl cinnamate

^{1}H NMR (400 MHz, $CDCl_3$) δ 3.74 (s, 3H), 6.38 (d, 1H, ^3J = 16.4 Hz), 7.31-7.33 (m, 3H), 7.45-7.47 (m, 2H), 7.63 (d, 1H, ^3J = 16.4 Hz) ppm.

(E)-n-Butyl cinnamate

^{1}H NMR (400 MHz, $CDCl_3$), δ 0.88 (t, 3H, ^3J = 7.6 Hz), 1.33-1.40 (m, 2H), 1.59-1.65 (m, 2H), 4.13 (t, 2H, ^3J = 6.8 Hz), 6.36 (d, 1H, ^3J = 16.0 Hz), 7.29-7.30 (m, 3H), 7.43-7.45 (m, 2H), 7.60 (d, 1H, ^3J = 16.4 Hz) ppm.

(E)-n-Butyl 3-(4-chlorophenyl) acrylate

^{1}H NMR (400 MHz, $CDCl_3$), δ 0.90 (t, 3H, ^3J = 7.2 Hz), 1.34-1.39 (m, 2H), 1.57-1.64 (m, 2H), 4.14 (t, 2H, ^3J = 6.8 Hz), 6.64 (d, 1H, ^3J = 16.0 Hz), 7.45 (d, 2H, ^3J = 8.0 Hz), 7.63 (d, 1H, ^3J = 16.0 Hz), 7.74 (d, 2H, ^3J = 8.0 Hz) ppm.

3. Results and discussion

3.1. Catalyst synthesis and characterization

At first, γ-Fe_2O_3 NPs were synthesized by a chemical co-precipitation technique of ferric and ferrous ions in alkali solution [33,34]. The magnetic nanoparticles were then allowed to react with an appropriate concentration of 3-chloropropyl trimethoxysilane to give chloro-functionalized γ-Fe_2O_3. The obtained chloro-functionalized γ-Fe_2O_3 was reacted with DABCO to produce γ-Fe_2O_3 supported with DABCO (DABCO-γ-Fe_2O_3). To this end, the reaction of DABCO-γ-Fe_2O_3 with $Pd(OAc)_2$ in dry acetone led to the formation of palladium-DABCO complex supported on γ-Fe_2O_3 MNPs (Pd-DABCO-γ-Fe_2O_3) (Scheme 1).

Scheme 1

The size and structure of Pd-DABCO-γ-Fe_2O_3 were evaluated using scanning electron microscopy (SEM) and high resolution transmission electron microscopy (HRTEM). The SEM image and HRTEM (Figure 1) showed uniformity and spherical-like morphology of nanoparticles with an average diameter from ∼50 to 60 and 17±5 nm, respectively.

Figure 1

FT-IR spectra of γ-Fe_2O_3, DABCO-γ-Fe_2O_3 and Pd-DABCO-γ-Fe_2O_3 were shown in Figure 2. The band at around 627–648 cm^{-1} was assigned to the stretching vibrations of Fe-O bond in these compounds [35]. The peaks positioned at 2910, 2930 and 1475 cm^{-1} in the FT-IR spectrum of DABCO-γ-Fe_2O_3 and Pd-DABCO-γ-Fe_2O_3 were related to the stretching and bending of the CH_2 bonds, respectively [18]. Si–O stretching bond was observed at about 1000–1110 cm^{-1} [18]. The anchoring of DABCO on γ-Fe_2O_3 was evidenced by the presence of $C–N^+$ stretching at 1615 cm^{-1} in the spectra of DABCO-γ-Fe_2O_3 and Pd-DABCO-γ-Fe_2O_3 [18]. In the spectrum of Pd-DABCO-γ-Fe_2O_3, new peaks appeared at 1360 and 1600 cm^{-1} for COO (in acetate) [36], and at 1400 and 1640 cm^{-1} for COO (in bridged acetate) and confirmed the presence of Pd in the catalyst [37].

Figure 2

The reflection planes of (2 2 0), (3 1 1), (4 0 0), (4 2 2), (5 1 1) and (4 4 0) at around 2θ = 30.4°, 35.8°, 43.6°, 53.7°, 57.6°, 63.2° were readily recognized from the XRD pattern of γ-Fe_2O_3 and Pd-DABCO-γ-Fe_2O_3 (Figure 3). The observed diffraction peaks agree with the cubic structure of maghemite (JCPDS file No 04-0755). The same set of characteristic peaks was observed in the XRD pattern of Pd-DABCO-γ-Fe_2O_3, which indicates the stability of the crystalline phase of nanoparticles during the subsequent surface modification. The average crystallite size of Pd-DABCO-γ-Fe_2O_3 (16 nm) was estimated using the Debye-Scherrer formula. It is important to note that XRD results gave little meaningful data for palladium immobilization on γ-Fe_2O_3 due to the low palladium loading on the support [38].

Figure 3

In the X-ray photoelectron spectrum (XPS) of Pd-DABCO-γ-Fe_2O_3, binding energies at 338.5 and 343.0 eV corresponding to Pd 3$d_{5/2}$ and Pd 3$d_{3/2}$, respectively, confirmed the presence of Pd (II) in the catalyst (Figure 4). XPS analysis of Pd-DABCO-γ-Fe_2O_3 after the Mizoroki-Heck cross-coupling reaction showed almost identical patterns of Pd (II) in Pd-DABCO-γ-Fe_2O_3 (Figure 5). No peaks corresponding to Pd (0) in the metallic state was detected.

Figure 4

Figure 5

The Pd content of Pd-DABCO-γ-Fe_2O_3 was determined by inductively coupled plasma (ICP). The ICP analysis showed that 0.16 mmol of Pd was anchored on 1.0 g of Pd-DABCO-γ-Fe_2O_3.

The thermogravimetric analysis (TGA) of Pd-DABCO-γ-Fe_2O_3 was used to determine the thermal stability and content of organic functional groups on the surface of MNPs (Figure 6). The small amount of weight loss around 100 ^oC was attributed to the desorption of adsorbed water. Another mass loss appeared at around 220 ^oC and the organic parts decomposed completely at 380 ^oC. According to the TGA profile, the amount of organic components supported on γ-Fe_2O_3 is estimated to be 0.14 $mmol.g^{-1}$. These results are in good agreement with the elemental analysis data (N = 0.40% and C = 2.42%).

Figure 6

The magnetization curves of Pd-DABCO-γ-Fe_2O_3 and γ-Fe_2O_3 were measured at room temperature using a vibrating sample magnetometer (VSM). No reduced remanence and coercivity were detected, indicating both unmodified and Pd-DABCO-γ-Fe_2O_3 are superparamagnetic (Figure 7). The value of saturation magnetic moments of γ-Fe_2O_3 and Pd-DABCO-γ-Fe_2O_3 are 68.5 and 60.3 emu/g, respectively.

Figure 7

3.2. Evaluation of catalytic activity of Pd-DABCO-γ-Fe_2O_3 in the Mizoroki-Heck cross-coupling reaction

Initially, the Mizoroki-Heck cross-coupling reaction of iodobenzene with *n*-butyl acrylate in the presence of Pd-DABCO-γ-Fe_2O_3 (1 mol%) was chosen as a model for optimizing reaction parameters such as the base and solvent at 100 °C (Scheme 2, Table 1). Among the examined bases, triethylamine (Et_3N) showed the best results for this reaction in terms of reaction time and yield (Entries 1-4). The importance of the base was shown by performing the reaction in the absence of the base. The results showed that under these conditions, a trace amount of the desired cross-coupling product was obtained after 24 h (Entry 5). The model reaction was also examined in several solvents including DMF, H_2O, EtOH, CH_3CN, $CHCl_3$ and toluene (Entries 6-11) and the best yield was obtained in DMF as solvent (Entry 6). To avoid the use of toxic and expensive organic solvents, the reaction was studied under solvent-free conditions. It was observed that the coupling reaction gave excellent yield of the product in 0.5 h (Entry 1). The yield of the product in a similar reaction at 80 °C was decreased to 80% (Entry 12). Coupling reactions did not take place in the absence of the catalyst or in the presence of γ-Fe_2O_3 and DABCO-γ-Fe_2O_3 even after 24 h (Entries 13-15). The catalytic activity of Pd-DABCO-γ-Fe_2O_3 was also higher than that of Pd-supported γ-Fe_2O_3 (Pd/γ-Fe_2O_3) as a catalyst (Entry 16).

Scheme 2

Table 1

The reaction of aryl halides with olefins in the presence of Pd-DABCO-γ-Fe_2O_3 under the best reaction conditions was then investigated (Table 2).

Table 2

The catalyst was effective for coupling reactions of olefins and iodobenzene to give the corresponding products in excellent yields (Table 2, Entries 1-4). Iodobenzene functionalized with electron-withdrawing or electron-donating substituents reacted with olefins rapidly and generated the corresponding products in high yields (Entries 5 and 6). This catalytic system was also successfully applied for the coupling reaction of substituted aryl bromides with *n*-butyl acrylate (Entries 7-10). Various aryl chlorides underwent the coupling reactions with *n*-butyl acrylate and gave the desired products in relatively good yields. However, the reaction proceeded in longer reaction time compared with aryl bromides and iodides (Entries 11-15).

It is worth to note that $^{3}J_{\text{H-H}}$ value of 16 Hz for vinyllic hydrogens of (E)-methyl cinnamate, (E)-*n*-butyl cinnamate and (E)-*n*-butyl 3-(4-chlorophenyl) acrylate was obtained using ^{1}H NMR spectra and showed an excellent selectivity for the formation of *trans* isomer of the products. The Mizoroki-Heck cross-coupling reactions of aryl halides with styrene were also examined. The corresponding products were obtained in 61-87% yields in 1–8 h (Entries 16-21).

The magnetic property of Pd-DABCO-γ-Fe_2O_3 facilitates efficient recovery of the catalyst from the reaction mixture during work-up procedure. After performing the cross-coupling reaction of iodobenzene with *n*-butyl acrylate under the present conditions, EtOAc was added to the reaction mixture. The catalyst was separated by an external magnet from the reaction mixture (Figure 8b), washed with EtOAc, dried 30 min at 100 ^{o}C and reused for a consecutive run under the same reaction conditions. The average isolated yield of the product for five consecutive runs was 90%, which clearly demonstrates the practical reusability of this catalyst (Figure 9).

Figure 8

Figure 9

4. Conclusions

In summary, palladium-DABCO complex supported on γ-Fe_2O_3 magnetic nanoparticles as a new phosphine-free palladium catalyst was synthesized and applied as a magnetically recyclable heterogeneous catalyst for Mizoroki-Heck cross-coupling reaction of aryl halides with olefins under solvent-free conditions. The catalyst was easily isolated from the reaction mixture by an external magnet and reused at least five times without significant degradation in its activity.

Acknowledgements

We are thankful to University of Birjand Research Council for their support on this work.

Reference

[1] S. Yahiaoui, A. Fardost, A. Trejos, M. Larhed, J. Org. Chem. 76 (2011) 2433-2438.

[2] D. S. Surry, S. L. Buchwald, Angew. Chem. 120 (2008) 6438-6461; Angew. Chem. Int. Ed. 47 (2008) 6338-6361.

[3] H. Doucet, J.-C. Hierso, Angew. Chem. 119 (2007) 850–888; Angew. Chem. Int. Ed. 46 (2007) 834-871.

[4] C. Torborg, M. Beller, Adv. Synth. Catal. 351 (2009) 3027-3043.

[5] Y.-J. Shang, J.-W. Wu, C.-L. Fan, J.-S. Hu, B.-Y. Lu, J. Organomet. Chem. 693 (2008) 2963-2966.

[6] C. Cao, Y. Zhuang, J. Zhao, Y. Peng, X. Li, Z. Shi, G. Pang, Y. Shi, Inorg. Chim. Acta 363 (2010) 3914-3918.

[7] J. Feng, C. Cai, J. Fluorine Chem. 146 (2013) 6–10.

[8] Y. Xue, Z. F. Fei, D. B. Zhao, Y. D. Li, Inorg. Chem. 47 (2008) 3292-3297.

[9] J. H. Cho, K.H. Shaughnessy, Synlett (2011), 2963-2966.

[10] A. Suzuki, in: D. Astruc (Ed.), Modern Arene Chemistry, Wiley-VCH, Weinheim, 2003, pp. 53–106.

[11] A. De Mejere, F. Diederich, Metal-catalyzed Cross-coupling Reactions, Wiley-VCH, Weinheim, 2004.

[12] C. S. Consorti, F. R. Flores, J. Dupont, J. Am. Chem. Soc.127 (2005) 12054-12065.

[13] X. Ma, Y. Zhou, J. Zhang, A. Zhu, T. Jiang. B. Han, Green Chem. 10 (2008) 59-66.

[14] R. Wang, B. Twamley, J. M. Shreeve, J. Org. Chem. 71 (2006) 426-429.

[15] R. Tao, S. Miao, Z. Liu, Y. Xie, B. Han, G. An, K. Ding, Green Chem. 11 (2009) 96-101.

[16] G. Liu, M. Hou, J. Song, T. Jiang, H. Fan, Z. Zhang, B. Han, Green Chem. 12 (2010) 65-69.

[17] S. Luo, X. Zheng, H. Xu, X. Mi, L. Zhang, J.-P. Cheng, Adv. Synth. Catal. 349 (2007) 2431-2434.

[18] A. Hasaninejad, M. Shekouhy, N. Golzar, A. Zare, M. M. Doroodmand, Appl. Catal. A: Gen. 402 (2011) 11-22.

[19] F. R. Fronczek, M. Ivie, A. W. Mawrick, Acta Cryst. C 46 (1990) 2057-2062.

[20] B. Twamley, O.D. Gupta, J. M. Shreeve, Acta Cryst. E 58 (2002) m663-m665.

[21] J.-H. Li, X.-C. Hu, Y.-X. Xie, Tetrahedron Lett. 47 (2006) 9239-9243.

[22] A. Kumbhar, S. Kamble, S. Jadhav, G. Rashinkar, R. Salunkhe, Catal. Lett. 142 (2012) 1388–1396.

[23] Y. Xu, Z. Zhang, J. Zheng, Q. Du, Y. Li, Appl. Organomet. Chem. 27 (2013), 13-18.

[24] H. Li, M. Yang, Q. Pu, Micropor. Mesopor. Mat.148 (2012) 166-173.

[25] S. Sobhani, S. Rezazadeh, Synlett (2010) 1485-1488.

[26] R. Malakooti, S. Sobhani, N. Razavi, S. Shafiei, R. Mokhtari, Collect. Czech. Chem. Commun. 76 (2011) 1979-1990.

[27] S. Sobhani, S. Rezazadeh, J. Iran. Chem. Soc. 8 **(**2011) 198-203.

[28] S. Sobhani, Z. Pakdin-Parizi, S. Rezazadeh, J. Organomet. Chem. 696 (2011) 813-817.

[29] S. Sobhani, Z. Pakdin-Parizi, N. Razavi, Appl. Catal. A: Gen. 409-410 (2011) 162-166.

[30] S. Sobhani, R. Jahanshahi, New J. Chem. 37 (2013) 1009-1015.

[31] S. Sobhani, M. Bazrafshan, A. Arabshahi Delluei, Z. Pakdin-Parizi, Appl. Catal. A: Gen. 454 (2013) 145-151.

[32] S. Sobhani, Z. Pakdin-Parizi, R. Naseri., J. Chem. Sci. 125 (2013) 975–979.

[33] B. Z. Tang, Y. Geng, J. W. Y. Lam, B. Li, X. Jing, X. Wang, F. Wang, A. B. Pakhomov, X. X. Zhang, Chem. Mater. 11 (1999) 1581-1589.

[34] K. M. Ho, P. Li, Langmuir 24 (2008) 1801-1807.

[35] N. Anand, K. H. P. Reddy, T. Satyanarayana, K. S. R. Rao, D. R. Burri, Catal. Sci. Technol. 2 (2012) 570–574.

[36] K. Mukhopadhyay, B. R. Sarkar, R. V. Chaudhari, J. Am. Chem. Soc. 124 (2002) 9692-9693.

[37] K. Sarkar, M. Nandi, M. Islam, M. Mubarak, A. Bhaumik, Appl. Catal. A: Gen. 352 (2009) 81–86.

[38] K. Karami, M. Bahrami Shehni, N. Rahimi, Appl. Organometal. Chem. 27 (2013) 437–443.

[39] M. L. Kantam, S. Roy, M. Roy, M. S. Subhas, P. R. Likhar, B. Sreedhar, B. M. Houdary, Synlett (2006) 2747–275.

[40] B. K. Allam, K. N. Singh, Synthesis (2011) 1125–1131.

[41] R. Bernini, S. Cacchi, G. Fabrizi, G. Forte, F. Petrucci, A. Prastaro, S. Niembro, A. Shafird, A. Vallribera, Green Chem. 12 (2010) 150–158.

[42] A. R. Hajipour, K. Karami, A. Pirisedigh, Appl. Organometal. Chem. 23 (2009) 504–511.

[43] H. Firouzabadi, N. Iranpoor, F. Kazemi, M. Gholinejad, J. Mol. Catal. A: Chem. 357 (2012) 154-161.

[44] N. Iranpoor, H. Firouzabadi, R. Azadi, Eur. J. Org. Chem. (2007) 2197-2201.

[45] R. Trivedi, S. Roy, M. Roy, B. Sreedhar, M. L. Kantam, New J. Chem. 31 (2007) 1575-1578.

[46] Y.-M. Liu, Y.-C. Lin, W.-C. Chen, J.-H. Cheng, Y.-L. Chen, G. P. A. Yap, S.-S. Sun, T.-G. Ong, Dalton Trans. 41 (2012) 7382–7389.

[47] N. Iranpoor, H. Firouzabadi, S. Motevalli, M. Talebi, J. Organomet. Chem. 708-709 (2012) 118-124.

[48] M. Amini, M. Bagherzadeh, S. Rostamnia, Chin. Chem. Lett. 24 (2013) 433–436.

[49] N. Iranpoor, H. Firouzabadi, A. Tarassoli, M. Fereidoonnezhad, Tetrahedron 66 (2010) 2415-2421.

[50] A. R. Hajipour, K. Karami, A. Pirisedigh, A. E. Ruoho, J. Organomet. Chem. 694 (2009) 2548–2554.

[51] C. Cao, Y. Li, Y. Li, G. Liu, Y. Shi, S. Wang, G. Pang, Y. Shi, Tetrahedron 69 (2013) 6241-6250.

[52] A. Kamal, V. Srinivasulu, B. N. Seshadri, N. Markandeya, A. Alarifi, N. Shankaraiah, Green Chem. 14 (2012) 2513-2522.

[53] A. Slamani, S. Demir, İ. Özdemir, Catal. Commun. 29 (2012) 141–144.

[54] B. Tamami, F. Farjadian, S. Ghasemi, H. Allahyari, New J. Chem. 37 (2013) 2011-2018.

Figure captions

Figure 1. SEM images (a, b) and HRTEM images (c, d, e) of Pd-DABCO-γ-Fe_2O_3

Figure 2. FT-IR spectra of γ-Fe_2O_3, DABCO-γ-Fe_2O_3 and Pd-DABCO-γ-Fe_2O_3

Figure 3. XRD patterns of a) γ-Fe_2O_3 and b) Pd-DABCO-γ-Fe_2O_3

Figure 4. X-ray photoelectron spectroscopy (XPS) of fresh Pd-DABCO-γ-Fe_2O_3

Figure 5. X-ray photoelectron spectroscopy (XPS) of used Pd-DABCO-γ-Fe_2O_3

Figure 6. TGA diagram of Pd-DABCO-γ-Fe_2O_3

Figure 7. Magnetization curves of γ-Fe_2O_3 and Pd-DABCO-γ-Fe_2O_3

Figure 8. a) Reaction mixture, b) Separation of Pd-DABCO-γ-Fe_2O_3 from the reaction mixture by an external magnet

Figure 9. Reusability of Pd-DABCO-γ-Fe_2O_3 as a magnetically recyclable heterogeneous catalyst for the Mizoroki–Heck cross-coupling reaction of iodobenzene with *n*-buthyl acrylate at 100 °C in 0.5 h

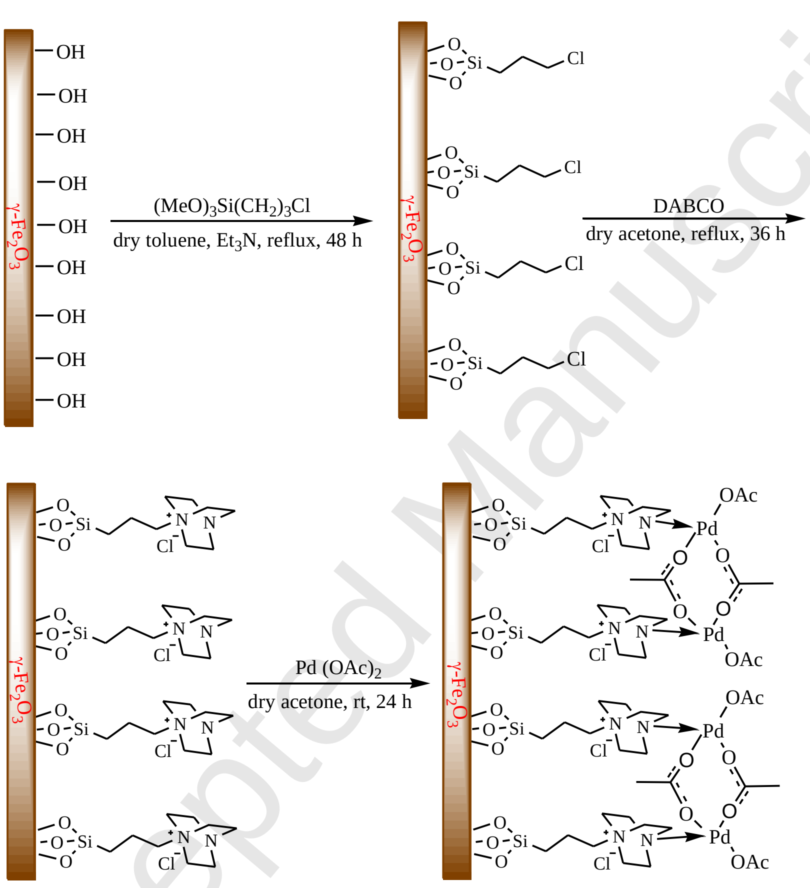

Scheme 1. Synthesis of Pd-DABCO-γ-Fe_2O_3

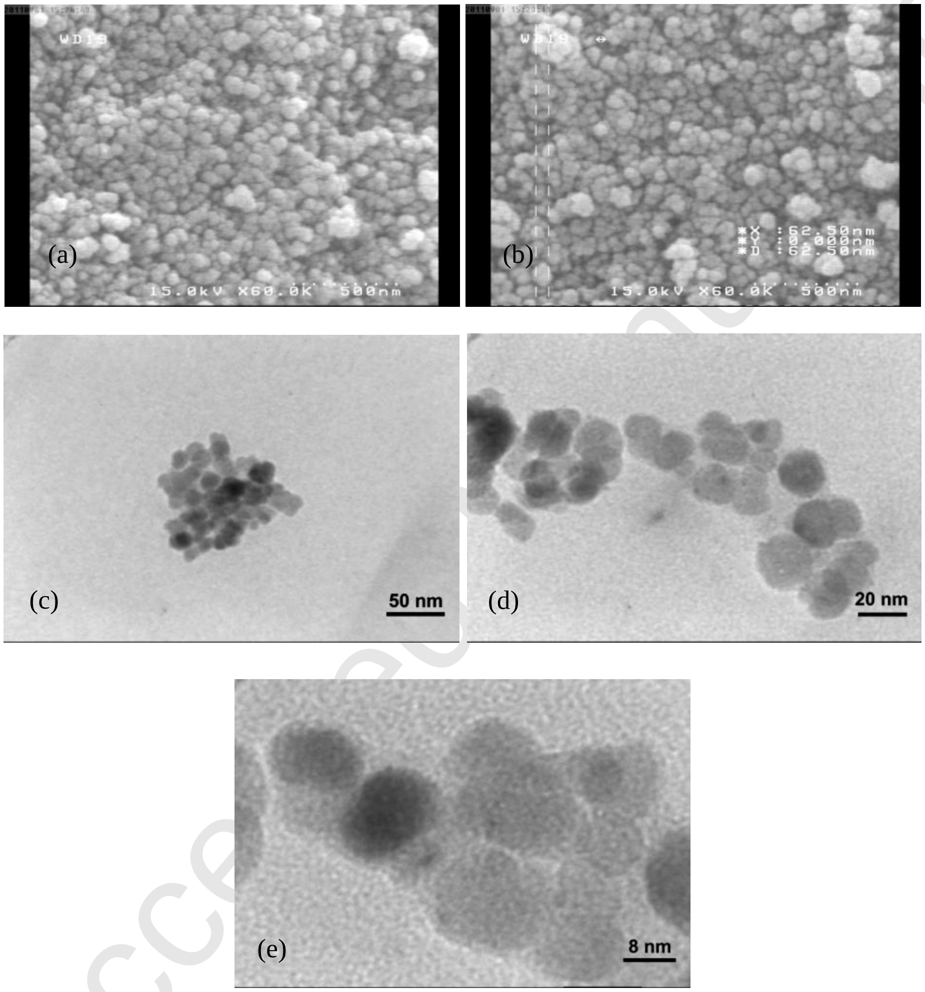

Figure 1. SEM images (a,b) and HRTEM images (c,d,e) of Pd-DABCO-γ-Fe_2O_3

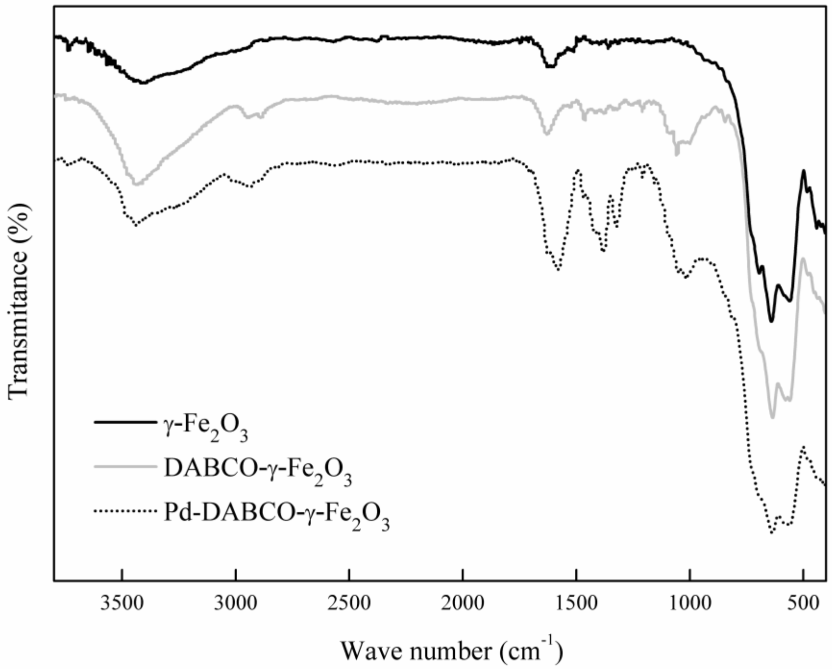

Figure 2. FT-IR spectra of γ-Fe_2O_3, DABCO-γ-Fe_2O_3 and Pd-DABCO-γ-Fe_2O_3

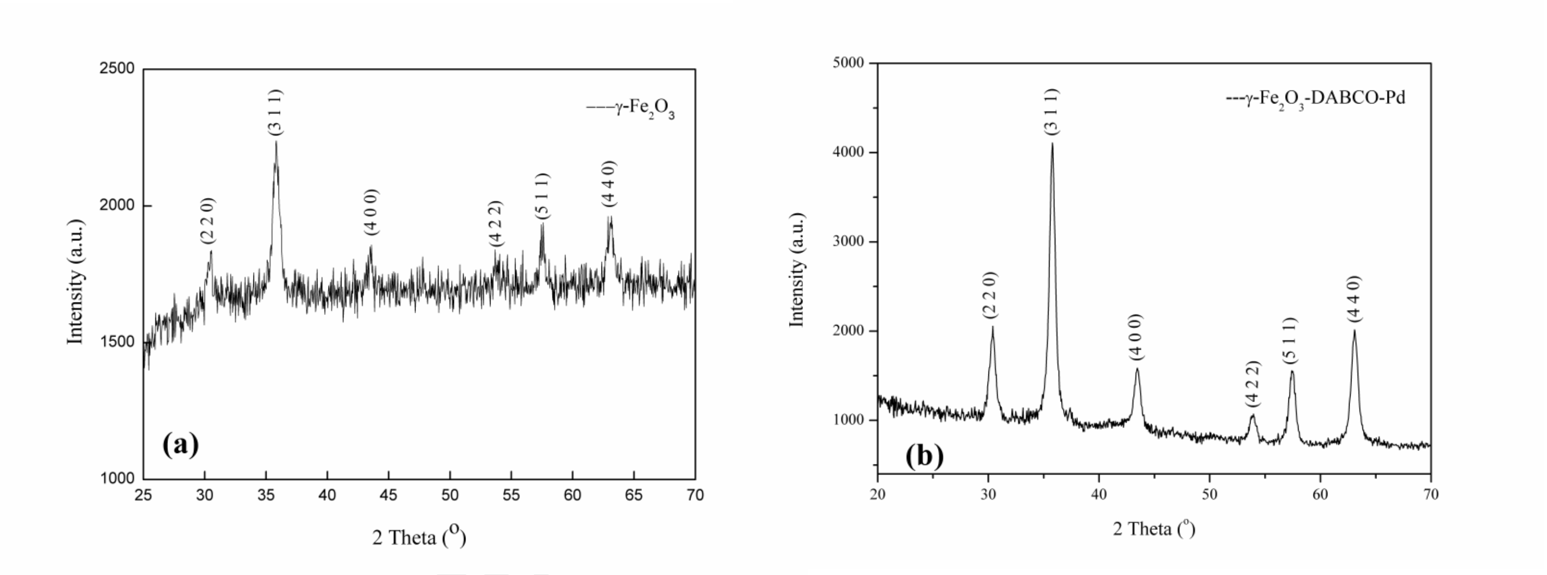

Figure 3. XRD patterns of a) γ-Fe_2O_3 and b) Pd-DABCO-γ-Fe_2O_3

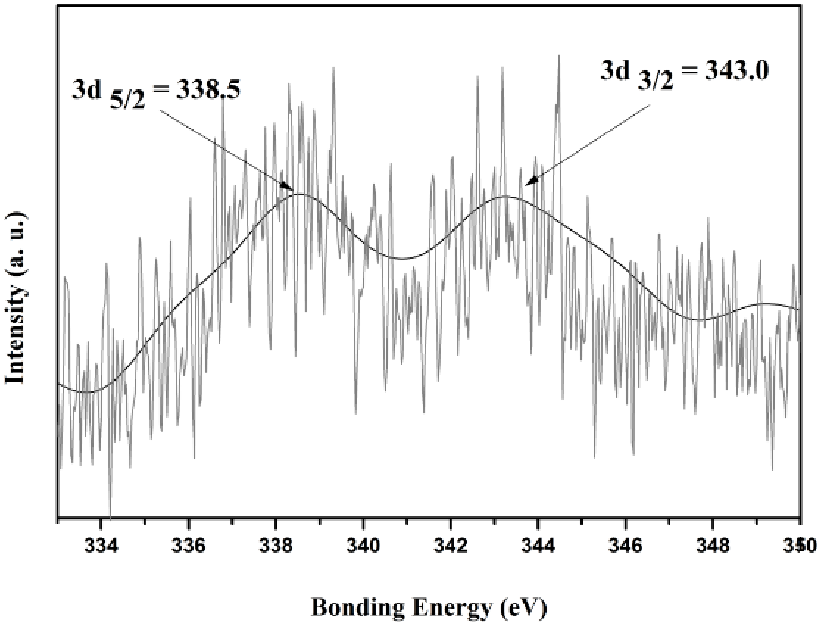

Figure 4. X-ray photoelectron spectroscopy (XPS) of fresh Pd-DABCO-γ-Fe_2O_3

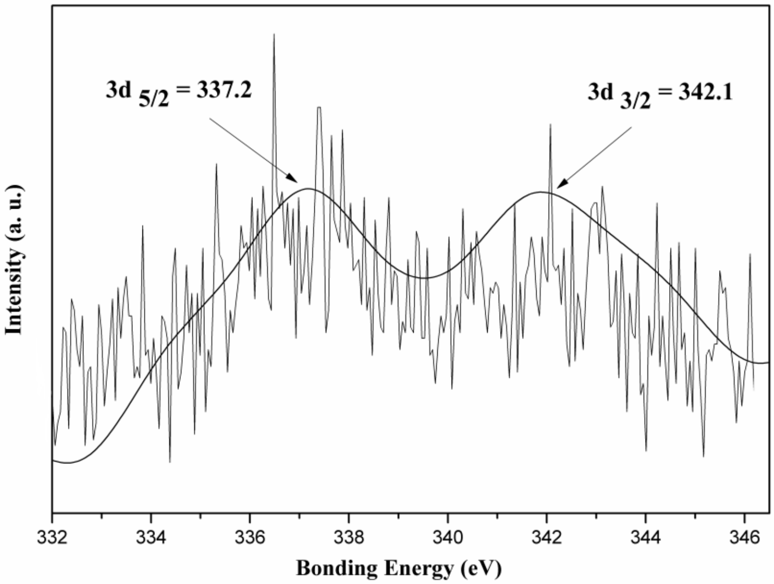

Figure 5. X-ray photoelectron spectroscopy (XPS) of used Pd-DABCO-γ-Fe_2O_3

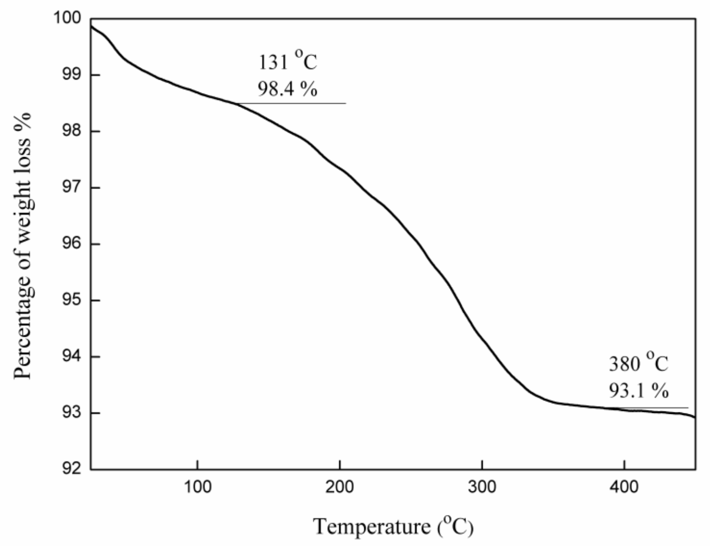

Figure 6. TGA diagram of Pd-DABCO-γ-Fe_2O_3

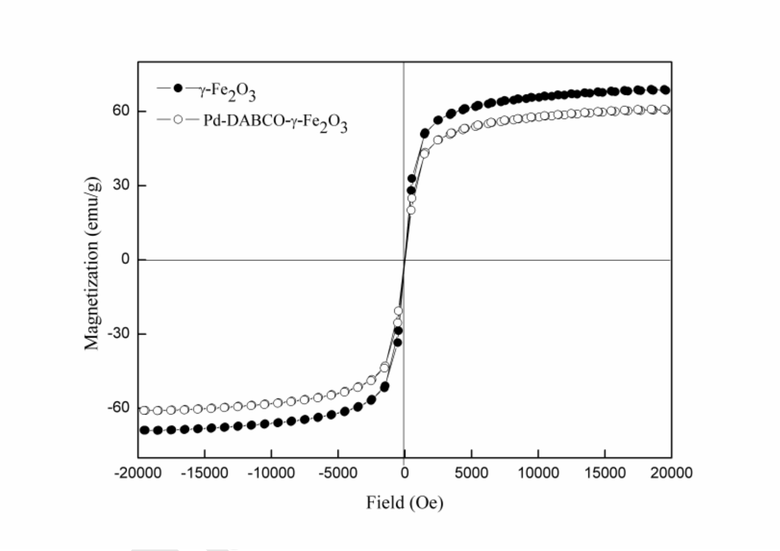

Figure 7. Magnetization curves of γ-Fe_2O_3 and Pd-DABCO-γ-Fe_2O_3

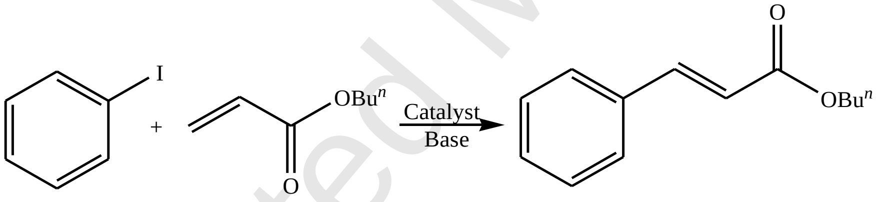

Scheme 2. Mizoroki-Heck cross-coupling reaction of iodobenzene with *n*-butyl acrylate

Table 1 Mizoroki–Heck cross-coupling reaction of iodobenzene with *n*-butyl acrylate under different conditions.

Entry	Iodobenzene: *n*-Butyl acrylate	Base	Solvent	Time (h)	Yield (%)[a]
1	1:1.1	Et_3N	-	0.5	92
2	1:1.1	K_2CO_3	-	2	70
3	1:1.1	KOH	-	2	81
4	1:1.1	NaOAC	-	2	74
5	1:1.1	-	-	24	Trace
6	1:1.1	Et_3N	DMF	0.5	96
7	1:1.1	Et_3N	H_2O	3	49
8	1:1.1	Et_3N	EtOH	3	41
9	1:1.1	Et_3N	CH_3CN	3	53
10	1:1.1	Et_3N	$CHCl_3$	3	34
11	1:1.1	Et_3N	toluene	3	26
12[b]	1:1.1	Et_3N	-	0.5	80
13[c]	1:1.1	Et_3N	-	24	Trace
14[d]	1:1.1	Et_3N	-	24	Trace
15[e]	1:1.1	Et_3N	-	24	Trace
16[f]	1:1.1	Et_3N	-	1	64

[a] Isolated yield. Reaction conditions: Et_3N (2 equivalents), Pd-DABCO-γ-Fe_2O_3 (1 mol%, except for entries 12-14), temperature = 100 ^oC.

[b] Temperature: 80 °C.

[c] No catalyst.

[d] Catalyst: γ-Fe_2O_3 (0.04 g).

[e] Catalyst: DABCO- γ-Fe_2O_3 (1 mol%).

[f] Catalyst: Pd/γ-Fe_2O_3 (1 mol%).

Table 2 Mizoroki-Heck cross-coupling reaction of olefins with aryl halides in the presence of Pd-DABCO-γ-Fe_2O_3 as a catalyst at 100 °C.

Entry	Arylhalide	Olefin	Product	Time (h)	Yield (%)^{a}
1	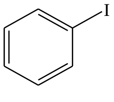	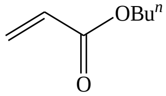	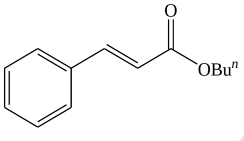	0.5	92
2	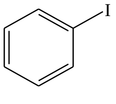	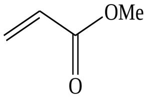	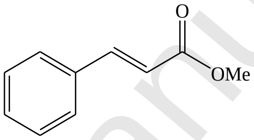	0.5	90
3	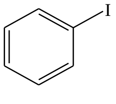	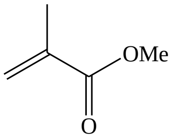	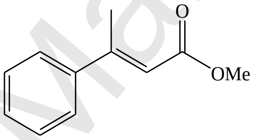	0.5	84
4	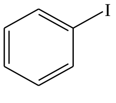	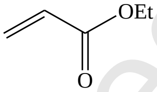	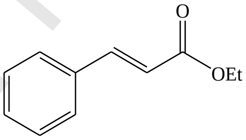	0.5	88
5	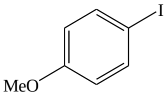	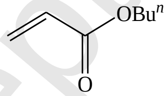	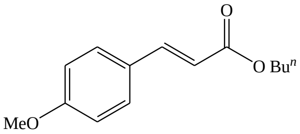	4	82
6	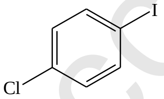	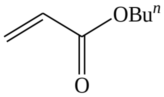	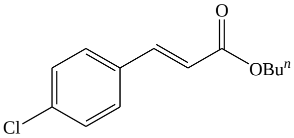	4	86
7	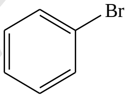	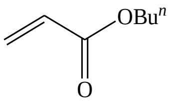	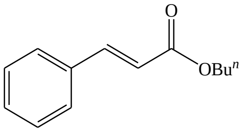	7	83^{b}
8	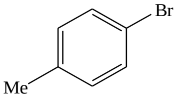	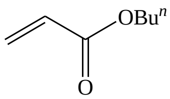	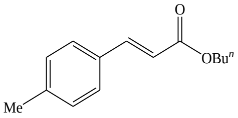	8	65$^{\mathbf{b}}$

9	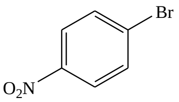	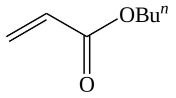	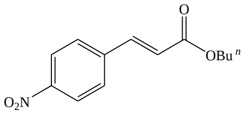	3	84
10	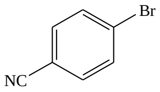	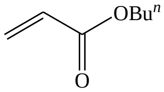	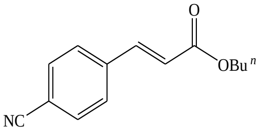	5	78
11	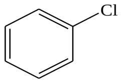	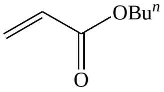	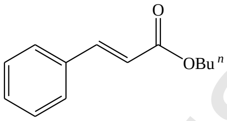	24	43[b]
12	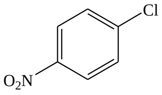	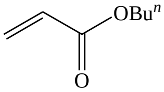	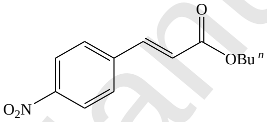	13	63[b]
13	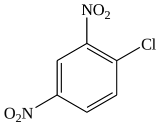	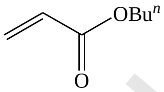	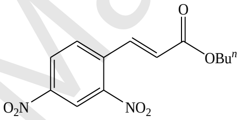	10	62[b]
14	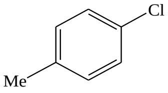	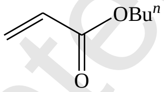	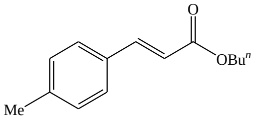	24	50[b]
15	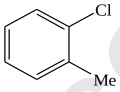	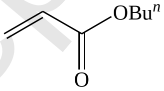	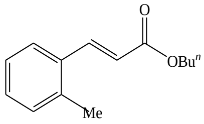	10	73[b]
16	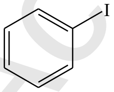	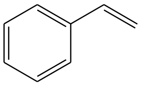	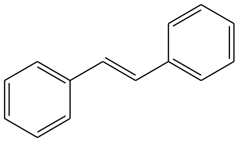	1	87
17	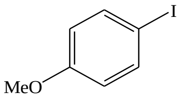	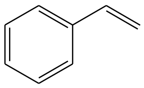	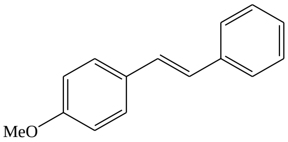	6	85
18	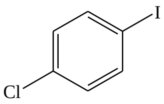	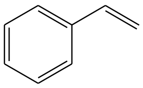	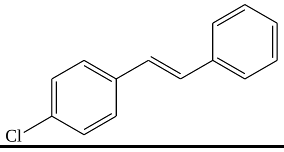	4	75

19	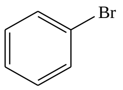	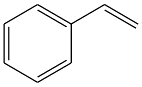	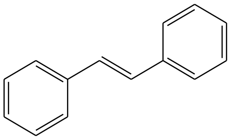	8	61[b]
20	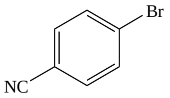	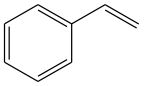	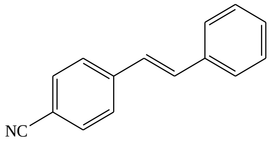	4	74[b]
21	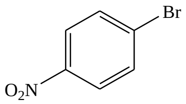	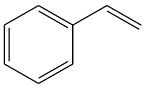	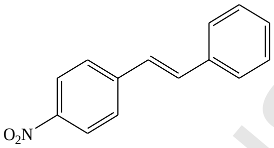	3	77[b]

[a] Isolated yield. Reaction conditions: aryl halide (1 mmol), olefin (1.1 mmol), Et_3N (2 mmol), catalyst (1 mol%, except for entries 7, 8, 11-15, 19-21). The products were characterized by comparison of their physical properties with the authentic samples [39-54].

[b] Catalyst = 3 mol%.

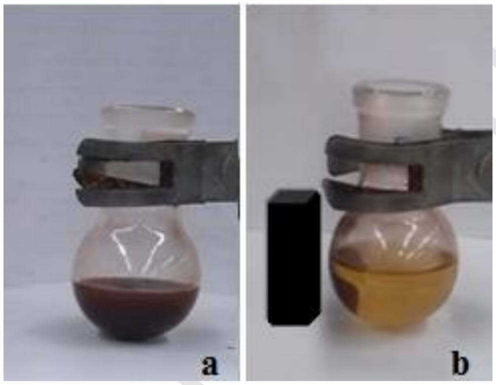

Figure 8. a) Reaction mixture, b) Separation of Pd-DABCO-γ-Fe_2O_3 from the reaction mixture by an external magnet

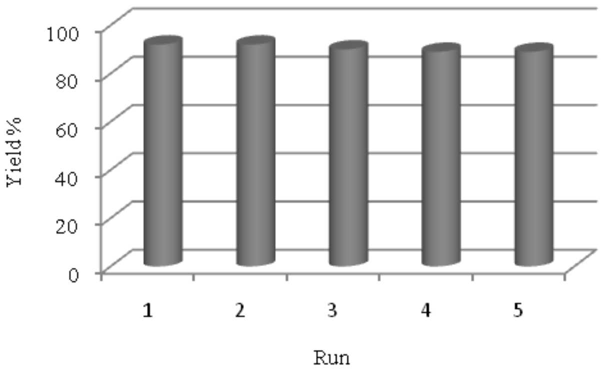

Figure 9. Reusability of Pd-DABCO-γ-Fe_2O_3 as a magnetically recyclable heterogeneous catalyst for the Mizoroki–Heck cross-coupling reaction of iodobenzene with *n*-buthyl acrylate at 100 °C in 0.5 h